Iterative Equalization for Single-Carrier Cyclic-Prefix in Doubly-Dispersive Channels

Philip Schniter and Hong Liu
Dept. EE, The Ohio State University, 2015 Neil Ave, Columbus, OH 43210
schniter.1@osu.edu, liu.523@osu.edu

***Abstract*— Single-carrier cyclic prefix (SCCP) has been proposed as an alternative to orthogonal frequency division multiplexing (OFDM). While the implementation complexity of the two schemes are comparable, SCCP avoids the peak-to-average power ratio problem that plagues OFDM. Both OFDM and SCCP receivers leverage the fast Fourier transform for computationally-efficient frequency-domain equalization. For channels that are significantly time-varying, however, frequency-domain equalization alone is inadequate. Several OFDM receiver modifications have been proposed for this time-varying case, including one which uses linear pre-processing and iterative estimation to yield excellent performance with low complexity. Here we design an SCCP receiver based on similar concepts.** [1]

I. Introduction

Orthogonal frequency division multiplexing (OFDM) [1], [2] has become a popular modulation format for digital communication in the presence of time-dispersive multipath. This is in large part due to the low complexity equalization afforded by OFDM's use of the fast Fourier transform (FFT). OFDM has the disadvantage of large peak-to-average power ratio (PAPR) relative to single-carrier systems, however, which leads to the requirement for expensive transmitter power amplifiers. Single-carrier cyclic prefix (SCCP) was proposed as an alternative to OFDM [3], [4]. Like OFDM, SCCP transmits blocks of data separated by guard intervals and leverages FFTs to accomplish frequency-domain equalization. Unlike OFDM, SCCP transmits QAM symbols, thereby circumventing the PAPR problem. Whereas OFDM uses one N-point FFT at the transmitter and another at the receiver, the SCCP employs two N-point FFTs at the receiver and none at the transmitter. Though SCCP's asymmetry may not be advantageous, its PAPR solution may be more important in some applications.

Fast circular convolution is an appropriate means of combating *time*-dispersive multipath fading, i.e., linear time-invariant (LTI) channels. For channels that are also *frequency*-dispersive, i.e., linear time-varying (LTV), circular convolution alone is not sufficient [5]–[7]. A number of authors have recently proposed modifications of OFDM for this doubly-dispersive environment (see, e.g., [8]–[12] and the references therein). In [12], $\mathcal{O}(N)$ low-complexity linear pre-processing was employed in conjunction with $\mathcal{O}(N)$ iterative estimation to yield excellent symbol estimation performance. This paper investigates the applicability of [12] to receivers for SCCP in doubly-selective channels. We shall see that, while many aspects of the OFDM modification [12] translate directly to SCCP, there are a number of important differences between the two systems.

[1]This work is supported in part by NSF CAREER Grant CCR-0237037.

In this extended abstract, we review the system model, summarize our preliminary work, and present preliminary results. We will use the following notation throughout: $(\cdot)^t$ denotes transpose, $(\cdot)^*$ conjugate, and $(\cdot)^H$ conjugate transpose. $\mathcal{C}(\boldsymbol{b})$ denotes a circulant matrix with first column $\boldsymbol{b}$, $\mathcal{D}(\boldsymbol{b})$ the diagonal matrix created from vector $\boldsymbol{b}$, $\boldsymbol{F}$ the unitary DFT matrix, $\boldsymbol{I}$ the identity matrix, and $\boldsymbol{i}_k$ the k^{th} column of $\boldsymbol{I}$. Expectation is denoted by $\mathrm{E}\{\cdot\}$, covariance by $\mathrm{Cov}\{\boldsymbol{b},\boldsymbol{c}\} := \mathrm{E}\{\boldsymbol{b}\boldsymbol{c}^H\} - \mathrm{E}\{\boldsymbol{b}\}\,\mathrm{E}\{\boldsymbol{c}^H\}$, element-wise multiplication by $\odot$, the Kronecker delta by $\delta(\cdot)$, and modulo-N by $\langle\cdot\rangle_N$.

II. System Model

We use $\boldsymbol{s} = [s_0, \ldots, s_{N-1}]^t$ to denote an N-block of (time-domain) finite-alphabet symbols that is cyclically prepended prior to transmission. The time-domain received N-vector, after removal of the guard interval which is assumed at least as long as the channel impulse response, can be written [3]

$$\boldsymbol{r} \;=\; \mathcal{H}_{\mathsf{tl}}\boldsymbol{s} + \boldsymbol{\nu}. \tag{1}$$

Here $\boldsymbol{\nu}$ contains i.i.d. zero-mean circular Gaussian noise samples (independent of $\boldsymbol{s}$) with variance σ^2, $\mathcal{H}_{\mathsf{tl}}$ is a (time-variant, circular) convolution matrix such that $[\mathcal{H}_{\mathsf{tl}}]_{n,l} = h_{\mathsf{tl}}(n, \langle n-l\rangle_N)$, and $h_{\mathsf{tl}}(n,l)$ is the response of the channel at time n to an impulse applied at time $n-l$. Time-domain windowing with coefficient vector $\boldsymbol{b}$ prior to the N-point DFT of $\boldsymbol{r}$ yields the "frequency-domain" observation $\boldsymbol{x}$:

$$\begin{aligned}\boldsymbol{x} \;&=\; \boldsymbol{F}\,\mathcal{D}(\boldsymbol{b})\mathcal{H}_{\mathsf{tl}}\boldsymbol{s} + \boldsymbol{F}\,\mathcal{D}(\boldsymbol{b})\boldsymbol{\nu} &(2)\\ &=\; \mathcal{C}(\boldsymbol{\beta})\boldsymbol{F}\mathcal{H}_{\mathsf{tl}}\boldsymbol{F}^H\boldsymbol{t} + \mathcal{C}(\boldsymbol{\beta})\boldsymbol{F}\boldsymbol{\nu} &(3)\\ &=\; \mathcal{C}(\boldsymbol{\beta})\mathcal{H}_{\mathsf{df}}\boldsymbol{t} + \mathcal{C}(\boldsymbol{\beta})\boldsymbol{w}, &(4)\end{aligned}$$

where we have used $\boldsymbol{t} := \boldsymbol{F}\boldsymbol{s}$, $\boldsymbol{w} := \boldsymbol{F}\boldsymbol{\nu}$, $\mathcal{H}_{\mathsf{df}} := \boldsymbol{F}\mathcal{H}_{\mathsf{tl}}\boldsymbol{F}^H$, $\boldsymbol{\beta} := \boldsymbol{F}\boldsymbol{b}/\sqrt{N}$ and the circulant matrix property $\mathcal{C}(\boldsymbol{g}) = \boldsymbol{F}\,\mathcal{D}(\sqrt{N}\boldsymbol{F}^H\boldsymbol{g})\boldsymbol{F}^H$.

Using the approach outlined in [12], $\boldsymbol{b}$ (or, equivalently, $\boldsymbol{\beta}$) can be designed to ensure that the matrix $\mathcal{C}(\boldsymbol{\beta})\mathcal{H}_{\mathsf{df}}$ approximates the banded structure illustrated in Fig. 1. Assuming wide-sense stationary uncorrelated scattering (WSSUS) [13], i.e., $\mathrm{E}\{h_{\mathsf{tl}}(n,l)h^*_{\mathsf{tl}}(n-q,l-m)\} = r_{\mathsf{t}}(q)\sigma_l^2\delta(m)$ where $r_{\mathsf{t}}(q)$ denotes the q-lag autocorrelation normalized so that $r_{\mathsf{t}}(0) = 1$ and σ_l^2 denotes the variance of the l^{th} tap, window coefficients

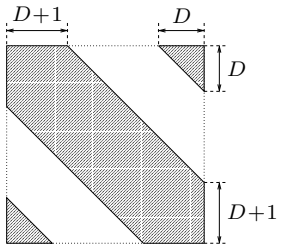

Fig. 1. Desired "banded" structure of matrix $\breve{\mathcal{H}} = \mathcal{C}(\boldsymbol{\beta})\mathcal{H}_{\mathsf{df}}$.

designed to maximize the signal to interference-plus-noise ratio (SINR) in $\boldsymbol{x}$ are given by (5)-(7) below [12]

$$\hat{\boldsymbol{b}}_\star \;=\; \boldsymbol{v}_\star\left(\boldsymbol{A}\odot\boldsymbol{R},\;\Big(\sigma^2+\sum_l \sigma_l^2\Big)\boldsymbol{I}-\boldsymbol{A}\odot\boldsymbol{R}\right) \quad (5)$$

$$[\boldsymbol{A}]_{m,n} \;:=\; \frac{\sin\big(\frac{\pi}{N}(2D+1)(n-m)\big)}{N\sin\big(\frac{\pi}{N}(n-m)\big)} \quad (6)$$

$$[\boldsymbol{R}]_{m,n} \;:=\; \sum_l \sigma_l^2\, r_{\mathsf{t}}(m-n), \quad (7)$$

where $\boldsymbol{v}_\star(\boldsymbol{B},\boldsymbol{C})$ denotes the principle generalized eigenvalue [14] of the matrix pair $(\boldsymbol{B},\boldsymbol{C})$. D is a design parameter typically chosen as $D=\lceil f_{\mathsf{d}}N\rceil+1$ when f_{d} is the (channel-use normalized) maximum Doppler frequency. Say that $\mathcal{C}(\boldsymbol{\beta})\mathcal{H}_{\mathsf{df}} = \mathcal{M}_{\mathrm{D}}\big(\mathcal{C}(\boldsymbol{\beta})\mathcal{H}_{\mathsf{df}}\big)+\overline{\mathcal{M}}_{\mathrm{D}}\big(\mathcal{C}(\boldsymbol{\beta})\mathcal{H}_{\mathsf{df}}\big)$, where $\mathcal{M}_{\mathrm{D}}(\cdot)$ is a mask operator which passes the elements in the shaded area of Fig. 1 and zeros the rest, and where $\overline{\mathcal{M}}_{\mathrm{D}}(\cdot)$ is the complement of $\mathcal{M}_{\mathrm{D}}(\cdot)$. With proper window design, we claim that $\overline{\mathcal{M}}_{\mathrm{D}}\big(\mathcal{C}(\boldsymbol{\beta})\mathcal{H}_{\mathsf{df}}\big)\approx\boldsymbol{0}$. Then, defining $\breve{\mathcal{H}} := \mathcal{M}_{\mathrm{D}}\big(\mathcal{C}(\boldsymbol{\beta})\mathcal{H}_{\mathsf{df}}\big)$ and $\boldsymbol{C}:=\mathcal{C}(\boldsymbol{\beta})$, we obtain the *approximate* system model (8):

$$\begin{cases}\boldsymbol{x}=\breve{\mathcal{H}}\boldsymbol{t}+\boldsymbol{C}\boldsymbol{w}\\ \boldsymbol{t}=\boldsymbol{F}\boldsymbol{s}.\end{cases} \quad (8)$$

III. Iterative Estimation

In this section we focus on the estimation of the finite-alphabet symbol vector $\boldsymbol{s}$ from $\boldsymbol{x}$ assuming (8) with known $\breve{\mathcal{H}}$. Though channel estimation is an important issue, we do not address it here for reasons of space. Our symbol estimation procedure, illustrated in Fig. 2, is iterative.

Given current guesses of the log-likelihood ratios (LLRs) of the symbols $\{s_k\}$ (which, on the first iteration, are set to zero), the means and variances of the elements in $\boldsymbol{s}$ are calculated as $\bar{\boldsymbol{s}}$ and $\boldsymbol{v}$, respectively. These are then transformed into the mean and covariance of $\boldsymbol{t}$. Using linear MMSE estimation and incorporating these mean/variance priors, the elements $\{t_k\}$ are estimated one-at-a-time, leveraging the banded structure of $\breve{\mathcal{H}}$ for complexity reduction. The resulting estimates $\hat{\boldsymbol{t}}$ are then transformed back into the $\boldsymbol{s}$-domain, from which the LLRs are updated. To accomplish this last step we assume a conditionally-Gaussian model for the estimates $\{\hat{s}_k\}$. The procedure then repeats, starting with the most recent LLRs. A more detailed description is given below. When appropriate, we use the superscript $^{(i)}$ to denote the i^{th} iteration.

Fig. 2. Iterative symbol estimation procedure.

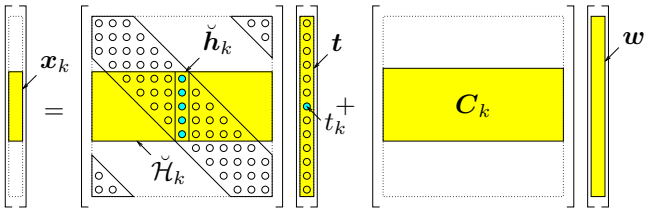

Fig. 3. Truncated observation model.

A. Linear Estimation with Priors

The banded structure of $\breve{\mathcal{H}}$ suggests that linear estimation of a particular element t_k might be accomplished with reasonable accuracy from the truncated observation $\boldsymbol{x}_k := [x_{k-D},\ldots,x_{k+D}]^t$, with indices taken modulo-N, as opposed to the full observation $\boldsymbol{x}$. (See Fig. 3.) We hope to realize substantial complexity reduction in doing so. Thus

$$\boldsymbol{x}_k \;=\; \breve{\mathcal{H}}_k\boldsymbol{t}+\boldsymbol{C}_k\boldsymbol{w} \;=\; \breve{\mathcal{H}}_k\boldsymbol{F}\boldsymbol{s}+\boldsymbol{C}_k\boldsymbol{w}, \quad (9)$$

where $\breve{\mathcal{H}}_k$ contains rows $\{k-D,\ldots,k+D\}$ of $\breve{\mathcal{H}}$ and $\boldsymbol{C}_k$ contains rows $\{k-D,\ldots,k+D\}$ of $\boldsymbol{C}$. The MMSE linear estimate of t_k given $\boldsymbol{x}_k$ is [15]

$$\hat{t}_k \;=\; \mathrm{E}\{t_k\}+\mathrm{Cov}(t_k,\boldsymbol{x}_k)\,\mathrm{Cov}(\boldsymbol{x}_k,\boldsymbol{x}_k)^{-1}(\boldsymbol{x}_k-\mathrm{E}\{\boldsymbol{x}_k\}) \quad (10)$$

Recalling $\mathrm{E}\{\boldsymbol{w}\}=\boldsymbol{0}$, $\mathrm{Cov}(\boldsymbol{w},\boldsymbol{w})=\sigma^2\boldsymbol{I}$, $\mathrm{Cov}(\boldsymbol{s},\boldsymbol{w})=\boldsymbol{0}$, assuming uncorrelated $\{s_k\}$, and defining $\bar{\boldsymbol{s}}:=\mathrm{E}\{\boldsymbol{s}\}$, $\mathcal{D}(\boldsymbol{v}):=\mathrm{Cov}(\boldsymbol{s},\boldsymbol{s})$, and $\bar{\boldsymbol{t}}:=\boldsymbol{H}\bar{\boldsymbol{s}}$, (10) becomes

$$\hat{t}_k \;=\; \bar{t}_k+\boldsymbol{g}_k^H(\boldsymbol{x}_k-\breve{\mathcal{H}}_k\bar{\boldsymbol{t}}) \quad (11)$$

$$\boldsymbol{g}_k \;:=\; \big(\breve{\mathcal{H}}_k\boldsymbol{F}\,\mathcal{D}(\boldsymbol{v})\boldsymbol{F}^H\breve{\mathcal{H}}_k^H+\sigma^2\boldsymbol{C}_k\boldsymbol{C}_k^H\big)^{-1}\breve{\mathcal{H}}_k\boldsymbol{F}\,\mathcal{D}(\boldsymbol{v})\boldsymbol{F}^H\boldsymbol{i}_k \quad (12)$$

from which estimates of $\boldsymbol{s}$ can be obtained as

$$\hat{\boldsymbol{s}} \;=\; \boldsymbol{F}^H\hat{\boldsymbol{t}} \quad\Leftrightarrow\quad \hat{s}_l \;=\; \boldsymbol{i}_l^H\boldsymbol{F}^H\sum_k \boldsymbol{i}_k\hat{t}_k. \quad (13)$$

B. A Conditionally Gaussian Model

Leveraging the finite-alphabet structure of the elements $\{s_k\}$ and assuming reasonably large N (to invoke the Central Limit Theorem), we assume that the estimation error is Gaussian, or, equivalently, that the estimates are conditionally Gaussian:

$$p(\hat{s}_l^{(i)}|s_l=b) \;=\; \frac{1}{\sigma_l^{(i)}(b)}\phi\left(\frac{\hat{s}_l^{(i)}-\mu_l^{(i)}(b)}{\sigma_l^{(i)}(b)}\right), \quad (14)$$

where $\phi(w) := \frac{1}{\sqrt{\pi}}e^{-w^2}$, $\mu_l^{(i)}(b) := \mathrm{E}\{\hat{s}_l^{(i)}|s_l=b\}$, and $[\sigma_l^{(i)}(b)]^2 := \mathrm{Cov}(\hat{s}_l^{(i)},\hat{s}_l^{(i)}|s_l=b)$. In the sequel, we restrict ourselves to the BPSK alphabet so that $b\in\{-1,+1\}$; QAM extensions are straightforward but tedious (see, e.g., [16]).

From (13) and the definition of $\mu_l^{(i)}(b)$,

$$\begin{aligned}\mu_l^{(i)}(b) &= \boldsymbol{i}_l^H \boldsymbol{F}^H \sum_k \boldsymbol{i}_k \,\mathrm{E}\{\hat{t}_k^{(i)}|s_l=b\} \\ &= \boldsymbol{i}_l^H \boldsymbol{F}^H \sum_k \boldsymbol{i}_k \Big(\bar{t}_k^{(i)} + \boldsymbol{g}_k^{(i)H}\big(\mathrm{E}\{\boldsymbol{x}_k|s_l=b\} - \breve{\mathcal{H}}_k \bar{\boldsymbol{t}}^{(i)}\big)\Big) \quad (15)\\ &= \bar{s}_l^{(i)} + \boldsymbol{i}_l^H \underbrace{\boldsymbol{F}^H \Big(\sum_k \boldsymbol{i}_k \boldsymbol{g}_k^{(i)H} \breve{\mathcal{H}}_k\Big) \boldsymbol{F}}_{:=\boldsymbol{Q}^{(i)H}} \boldsymbol{i}_l (b-\bar{s}_l^{(i)}) \\ &= \bar{s}_l^{(i)} + Q_{l,l}^{(i)*}(b-\bar{s}_l^{(i)}) \;=\; (1-Q_{l,l}^{(i)*})\bar{s}_l^{(i)} + Q_{l,l}^{(i)*} b \qquad (16)\end{aligned}$$

where in (15) we used the fact that $\mathrm{E}\{\boldsymbol{x}_k|s_l=b\} = \breve{\mathcal{H}}_k \boldsymbol{F}\big(\bar{\boldsymbol{s}}^{(i)} + \boldsymbol{i}_l(b-\bar{s}_l^{(i)})\big) = \breve{\mathcal{H}}_k \bar{\boldsymbol{t}}^{(i)} + \breve{\mathcal{H}}_k \boldsymbol{F} \boldsymbol{i}_l (b-\bar{s}_l^{(i)})$. Next we find an expression for $[\sigma_l^{(i)}(b)]^2$. Before doing so, however, it will be convenient to note from (11) and (13) that

$$\begin{aligned}\hat{s}_l^{(i)} &= \boldsymbol{i}_l^H \boldsymbol{F}^H \sum_k \boldsymbol{i}_k \Big(\bar{t}_k^{(i)} + \boldsymbol{g}_k^{(i)H}\big(\boldsymbol{x}_k - \breve{\mathcal{H}}_k \bar{\boldsymbol{t}}^{(i)}\big)\Big) \\ &= \boldsymbol{i}_l^H \boldsymbol{F}^H \sum_k \boldsymbol{i}_k \Big(\bar{t}_k^{(i)} + \boldsymbol{g}_k^{(i)H}\big(\breve{\mathcal{H}}_k \boldsymbol{F}\boldsymbol{s} + \boldsymbol{C}_k \boldsymbol{F}\boldsymbol{\nu} - \breve{\mathcal{H}}_k \boldsymbol{F}\bar{\boldsymbol{s}}^{(i)}\big)\Big) \\ &= \bar{s}_l^{(i)} + \boldsymbol{i}_l^H \boldsymbol{F}^H \Big(\sum_k \boldsymbol{i}_k \boldsymbol{g}_k^{(i)H} \breve{\mathcal{H}}_k\Big) \boldsymbol{F}(\boldsymbol{s}-\bar{\boldsymbol{s}}^{(i)}) \\ &\quad + \boldsymbol{i}_l^H \underbrace{\boldsymbol{F}^H \Big(\sum_k \boldsymbol{i}_k \boldsymbol{g}_k^{(i)H} \boldsymbol{C}_k\Big) \boldsymbol{F}}_{:=\boldsymbol{P}^{(i)H}} \boldsymbol{\nu} \\ &= \bar{s}_l^{(i)} + \boldsymbol{i}_l^H \boldsymbol{Q}^{(i)H}(\boldsymbol{s}-\bar{\boldsymbol{s}}^{(i)}) + \boldsymbol{i}_l^H \boldsymbol{P}^{(i)H}\boldsymbol{\nu} \\ &= \mu_l^{(i)}(b) + \boldsymbol{i}_l^H \boldsymbol{Q}^{(i)H}\big(\boldsymbol{s} - \bar{\boldsymbol{s}}^{(i)} + \boldsymbol{i}_l(\bar{s}_l^{(i)} - b)\big) + \boldsymbol{i}_l^H \boldsymbol{P}^{(i)H}\boldsymbol{\nu} \qquad (17)\end{aligned}$$

and that, since $\mathrm{E}\{\boldsymbol{s}|s_l=b\} = \bar{\boldsymbol{s}}^{(i)} - \boldsymbol{i}_l(\bar{s}_l^{(i)} - b)$,

$$\begin{aligned}&\mathrm{E}\Big\{\big(\boldsymbol{s} - \bar{\boldsymbol{s}}^{(i)} + \boldsymbol{i}_l(\bar{s}_l^{(i)}-b)\big)\big(\boldsymbol{s} - \bar{\boldsymbol{s}}^{(i)} + \boldsymbol{i}_l(\bar{s}_l^{(i)}-b)\big)^H | s_l=b\Big\} \\ &= \mathrm{Cov}(\boldsymbol{s},\boldsymbol{s}|s_l=b) \\ &= \mathcal{D}(\boldsymbol{v}^{(i)}) - \boldsymbol{i}_l \boldsymbol{i}_i^H v_l^{(i)}. \qquad (18)\end{aligned}$$

Using (17), (18), and the definition of $\sigma_l^{(i)}(b)$,

$$\begin{aligned}[\sigma_l^{(i)}(b)]^2 &= \mathrm{E}\Big\{\big(\hat{s}_l^{(i)} - \mu_l^{(i)}(b)\big)\big(\hat{s}_l^{(i)} - \mu_l^{(i)}(b)\big)^H | s_l=b\Big\} \\ &= \boldsymbol{i}_l^H \boldsymbol{Q}^{(i)H}\Big(\mathcal{D}(\boldsymbol{v}^{(i)}) - \boldsymbol{i}_l \boldsymbol{i}_l^H v_l^{(i)}\Big)\boldsymbol{Q}^{(i)}\boldsymbol{i}_l + \sigma^2 \boldsymbol{i}_l^H \boldsymbol{P}^{(i)H}\boldsymbol{P}^{(i)}\boldsymbol{i}_l \\ &= \boldsymbol{q}_l^{(i)H}\,\mathcal{D}(\boldsymbol{v}^{(i)})\boldsymbol{q}_l^{(i)} - |Q_{l,l}^{(i)}|^2 v_l^{(i)} + \sigma^2 \|\boldsymbol{p}_l^{(i)}\|^2 \qquad (19)\end{aligned}$$

where $\boldsymbol{q}_l^{(i)}$ denotes the l^{th} column of $\boldsymbol{Q}^{(i)}$ and where $\boldsymbol{p}_l^{(i)}$ denotes the l^{th} column of $\boldsymbol{P}^{(i)}$.

C. Log-Likelihood Ratio and Update of Priors

The *a priori* and *a posteriori* log likelihood ratio (LLR) are defined as $L(s_l) := \log\frac{P(s_l=+1)}{P(s_l=-1)}$ and $L(s_l|\hat{s}_l^{(i)}) := \log\frac{P(s_l=+1|\hat{s}_l^{(i)})}{P(s_l=-1|\hat{s}_l^{(i)})}$, respectively. The LLR update $\Delta(\hat{s}_l^{(i)}) := L(s_l|\hat{s}_l^{(i)}) - L(s_l)$ can be shown to equal

$$\begin{aligned}\Delta(\hat{s}_l) &= \log\frac{p(\hat{s}_l^{(i)}|s_l=+1)}{p(\hat{s}_l^{(i)}|s_l=-1)} \\ &= \frac{|\hat{s}_l^{(i)} - \mu_l^{(i)}(-1)|^2 - |\hat{s}_l^{(i)} - \mu_l^{(i)}(+1)|^2}{[\sigma_l^{(i)}(\pm 1)]^2} \\ &= 4\,\frac{\mathrm{Re}\big(Q_{l,l}^{(i)}(\hat{s}_l^{(i)} - \bar{s}_l^{(i)})\big) + |Q_{l,l}^{(i)}|^2 \bar{s}_l^{(i)}}{\boldsymbol{q}_l^{(i)H}\,\mathcal{D}(\boldsymbol{v}^{(i)})\boldsymbol{q}_l^{(i)} - |Q_{l,l}^{(i)}|^2 v_l^{(i)} + \sigma^2\|\boldsymbol{p}_l^{(i)}\|^2} \qquad (20)\end{aligned}$$

where we used the facts that $\sigma_l^{(i)}(+1) = \sigma_l^{(i)}(-1)$ and

$$\begin{aligned}&\big|\hat{s}_l^{(i)} - \mu_l^{(i)}(-1)\big|^2 - \big|\hat{s}_l^{(i)} - \mu_l^{(i)}(+1)\big|^2 \\ &= \big|\hat{s}_l^{(i)} - (1-Q_{l,l}^{(i)*})\bar{s}_l^{(i)} + Q_{l,l}^{(i)*}\big|^2 \\ &\quad - \big|\hat{s}_l^{(i)} - (1-Q_{l,l}^{(i)*})\bar{s}_l^{(i)} - Q_{l,l}^{(i)*}\big|^2 \\ &= 4\,\mathrm{Re}\big\{\big(\hat{s}_l^{(i)} - (1-Q_{l,l}^{(i)*})\bar{s}_l^{(i)}\big)Q_{l,l}^{(i)}\big\} \\ &= 4\,\mathrm{Re}\big\{Q_{l,l}^{(i)}(\hat{s}_l^{(i)} - \bar{s}_l^{(i)})\big\} + |Q_{l,l}^{(i)}|^2 \bar{s}_l^{(i)} \qquad (21)\end{aligned}$$

since we will have $\bar{s}_i \in \mathbb{R}$ with a BPSK alphabet.

Updating of the priors can be accomplished via

$$\bar{s}_l^{(i+1)} = \sum_{b\in\mathcal{B}} b\cdot P(s_l=b|\hat{s}_l^{(i)}) \;=\; \tanh\left(\frac{L(s_l|\hat{s}_l^{(i)})}{2}\right) \qquad (22)$$

$$v_l^{(i+1)} = \sum_{b\in\mathcal{B}} \big(b - \bar{s}_l^{(i+1)}\big)^2 P(s_l=b|\hat{s}_l^{(i)}) \;=\; 1 - (\bar{s}_l^{(i+1)})^2 \qquad (23)$$

We set the *a priori* LLR for iteration $i+1$ equal to the *a posteriori* LLR from iteration i. Denoting the *a priori* LLR used in iteration i by $L^{(i)}(s_l)$, we obtain the LLR update:

$$L^{(i+1)}(s_l) \;=\; L(s_l|\hat{s}_l^{(i)}) \;=\; L^{(i)}(s_l) + \Delta(\hat{s}_l^{(i)}). \qquad (24)$$

We should point out that a soft decoding algorithm could be easily embedded within the bottom path of Fig. 2 (e.g., [16]). If, on the other hand, hard symbol estimates are desired, they can be generated via $\hat{\hat{s}}_l^{(i)} = \mathrm{sign}\big(\mathrm{Re}(\hat{s}_l^{(i)})\big) = \mathrm{sign}\big(\bar{s}_l^{(i)}\big) = \mathrm{sign}\big(L(s_l|\hat{s}_l^{(i)})\big)$. An algorithm summary appears in Table I.

D. Efficient Implementation

Many of the quantities in the algorithm outlined in Table I have structures that lead to efficient computation.

$\boldsymbol{C}_k\boldsymbol{C}_k^H$ is a sub-block of $\boldsymbol{C}\boldsymbol{C}^H = \mathcal{C}(\boldsymbol{F}(\boldsymbol{b}\odot\boldsymbol{b}^*)/\sqrt{N})$, the latter of which requires $\mathcal{O}(N\log N)$ operations to compute. Furthermore, the Toeplitz nature of $\boldsymbol{C}\boldsymbol{C}^H$ implies that the subplot $\boldsymbol{C}_k\boldsymbol{C}_k^H$ is identical for every k. Thus, $\boldsymbol{C}_0\boldsymbol{C}_0^H$ can be calculated once and used for all iterations and all k.

Although $\breve{\mathcal{H}}_k$ is an $(2D+1)\times N$ matrix, it contains only $4D+1$ non-zero columns. Thus, calculation of $\breve{\mathcal{H}}_k\bar{\boldsymbol{t}}^{(i)}$ and $\breve{\mathcal{H}}_k^H\boldsymbol{g}_k^{(i)}$ require $\mathcal{O}(D^2)$ operations and must be done N times per iteration. Calculation of $\sum_{k=0}^{N-1}\breve{\mathcal{H}}_k^H\boldsymbol{g}_k^{(i)}\boldsymbol{i}_k^H$ requires $\mathcal{O}(ND^2)$ operations and must be done once per iteration. Calculation of $\boldsymbol{F}\,\mathcal{D}(\boldsymbol{v}^{(i)})\boldsymbol{F}^H$ requires $\mathcal{O}(N\log N)$ operations and must be done once per iteration. Given $\boldsymbol{F}\,\mathcal{D}(\boldsymbol{v}^{(i)})\boldsymbol{F}^H$, calculation of $\breve{\mathcal{H}}_k\boldsymbol{F}\,\mathcal{D}(\boldsymbol{v}^{(i)})\boldsymbol{F}^H\breve{\mathcal{H}}_k^H$ and $\breve{\mathcal{H}}_k\boldsymbol{F}\,\mathcal{D}(\boldsymbol{v}^{(i)})\boldsymbol{F}^H\boldsymbol{i}_k$ require $\mathcal{O}(D^3)$ and $\mathcal{O}(D^2)$ operations, respectively, for each k. Note that the matrix inverse used to compute $\boldsymbol{g}_k$ is performed

$L^{(0)}(s_l) = 0 \; \forall l$
for $i = 0 \ldots,$
  for $l = 0 \ldots N-1,$
    $\bar{s}_l^{(i)} = \tanh(L^{(i)}(s_l)/2)$
    $v_l^{(i)} = 1 - (\bar{s}_l^{(i)})^2$
  end
  $\bar{\boldsymbol{t}}^{(i)} = \boldsymbol{F}\bar{\boldsymbol{s}}^{(i)}$
  for $k = 0 \ldots N-1,$
    $\boldsymbol{g}_k^{(i)} = \left(\breve{\mathcal{H}}_k \boldsymbol{F}\,\mathcal{D}(\boldsymbol{v}^{(i)})\boldsymbol{F}^H \breve{\mathcal{H}}_k^H + \sigma^2 \boldsymbol{C}_k \boldsymbol{C}_k^H\right)^{-1} \breve{\mathcal{H}}_k \boldsymbol{F}\,\mathcal{D}(\boldsymbol{v}^{(i)})\boldsymbol{F}^H \boldsymbol{i}_k$
    $\hat{t}_k^{(i)} = \bar{t}_k^{(i)} + \boldsymbol{g}_k^{(i)H}(\boldsymbol{x}_k - \breve{\mathcal{H}}_k \bar{\boldsymbol{t}}^{(i)})$
  end
  $\boldsymbol{Q}^{(i)} = \boldsymbol{F}^H \Big(\sum_{k=0}^{N-1} \breve{\mathcal{H}}_k^H \boldsymbol{g}_k^{(i)} \boldsymbol{i}_k^H\Big)\boldsymbol{F}$
  $\boldsymbol{P}^{(i)} = \boldsymbol{F}^H \Big(\sum_{k=0}^{N-1} \boldsymbol{C}_k^H \boldsymbol{g}_k^{(i)} \boldsymbol{i}_k^H\Big)\boldsymbol{F}$
  $\hat{\boldsymbol{s}}^{(i)} = \boldsymbol{F}^H \hat{\boldsymbol{t}}^{(i)}$
  for $l = 0 \ldots N-1,$
    $L^{(i+1)}(s_l) = L^{(i)}(s_l) + 4\,\dfrac{\mathrm{Re}\{Q_{l,l}^{(i)}(\hat{s}_l^{(i)} - \bar{s}_l^{(i)})\} + |Q_{l,l}^{(i)}|^2 \bar{s}_l^{(i)}}{\boldsymbol{q}_l^{(i)H}\,\mathcal{D}(\boldsymbol{v}^{(i)})\boldsymbol{q}_l^{(i)} - |Q_{l,l}^{(i)}|^2 v_l^{(i)} + \sigma^2 \|\boldsymbol{p}_i\|^2}$
  end
end

TABLE I
SUMMARY OF ITERATIVE SYMBOL ESTIMATION ALGORITHM.

on a $(2D+1)\times(2D+1)$ matrix. Thus, for computation $\{\boldsymbol{g}_k^{(i)}\}$, we require $\mathcal{O}(ND^3)$ operations.

To update the likelihoods $\{L^{(i)}(s_k)\}_{k=0}^{N-1}$, we are especially interested in the computation of $\{\boldsymbol{q}_k^{(i)H}\,\mathcal{D}(\boldsymbol{v}^{(i)})\boldsymbol{q}_k^{(i)}\}_{k=0}^{N-1}$, $\{Q_{k,k}^{(i)}\}_{k=0}^{N-1}$, and $\{\|\boldsymbol{p}_k^{(i)}\|^2\}_{k=0}^{N-1}$. Direct computation of these quantities eliminates the need to explicitly compute $\boldsymbol{Q}^{(i)}$ and $\boldsymbol{P}^{(i)}$. For brevity we omit superscripts $^{(i)}$ in the sequel.

1) Computation of $\{\boldsymbol{q}_k^H\,\mathcal{D}(\boldsymbol{v})\boldsymbol{q}_k\}_{k=0}^{N-1}$: From the definition of $\boldsymbol{Q}$ and the results in the appendix, we know that

$$Q_{n,m} \;=\; \frac{1}{\sqrt{N}} \sum_{d=-2D}^{2D} e^{j\frac{2\pi}{N}nd} [\boldsymbol{F}\boldsymbol{a}_d]_{\langle m-n\rangle_N} \tag{25}$$

where $\boldsymbol{a}_d$ is the d^{th} sub-diagonal of $\sum_{k=0}^{N-1} \breve{\mathcal{H}}_k^H \boldsymbol{g}_k \boldsymbol{i}_k^H$, i.e., $[\boldsymbol{a}_d]_m = \big[\sum_{k=0}^{N-1} \breve{\mathcal{H}}_k^H \boldsymbol{g}_k \boldsymbol{i}_k^H\big]_{\langle d+m\rangle_N, m}$. Writing $\boldsymbol{\alpha}_d = \boldsymbol{F}\boldsymbol{a}_d$ and $\alpha_{d,m} = [\boldsymbol{\alpha}_d]_m$, we find

$$\boldsymbol{q}_k^H\,\mathcal{D}(\boldsymbol{v})\boldsymbol{q}_k \;=\; \sum_{n=0}^{N-1} |Q_{n,k}|^2 v_n \tag{26}$$

$$= \frac{1}{N} \sum_{n=0}^{N-1} v_n \sum_{d,l=-2D}^{2D} e^{-j\frac{2\pi}{N}n(l-d)} \alpha_{d,\langle k-n\rangle_N} \alpha_{l,\langle k-n\rangle_N}^* \tag{27}$$

$$= \frac{1}{N} \sum_{m=0}^{N-1} v_{\langle k-m\rangle_N} \sum_{d,l=-2D}^{2D} e^{-j\frac{2\pi}{N}(l-d)(k-m)} \alpha_{d,m} \alpha_{l,m}^* \tag{28}$$

where we used $m = \langle k-n\rangle_N$ so that $n = \langle k-m\rangle_N$. If we define $\beta_m(d,l) := \alpha_{d,m}\alpha_{l,m}^* e^{j\frac{2\pi}{N}(l-d)m}$ and $\boldsymbol{D}(d,l) := \mathcal{D}([e^{-j\frac{2\pi}{N}(l-d)\cdot 0}, \ldots, e^{-j\frac{2\pi}{N}(l-d)(N-1)}])$, then

$$\big[\boldsymbol{q}_0^H\,\mathcal{D}(\boldsymbol{v})\boldsymbol{q}_0,\; \boldsymbol{q}_1^H\,\mathcal{D}(\boldsymbol{v})\boldsymbol{q}_1,\; \ldots,\; \boldsymbol{q}_{N-1}^H\,\mathcal{D}(\boldsymbol{v})\boldsymbol{q}_{N-1}\big]^t$$

$$= \frac{1}{N} \sum_{d,l=-2D}^{2D} \boldsymbol{D}(d,l)\,\mathcal{C}(\boldsymbol{v})\boldsymbol{\beta}(d,l) \tag{29}$$

$$= \frac{1}{\sqrt{N}} \sum_{d,l=-2D}^{2D} \boldsymbol{D}(d,l)\boldsymbol{F}\,\mathcal{D}(\boldsymbol{F}^H\boldsymbol{v})\boldsymbol{F}^H\boldsymbol{\beta}(d,l) \tag{30}$$

Thus computation of $\{\boldsymbol{q}_k^H\,\mathcal{D}(\boldsymbol{v})\boldsymbol{q}_k\}_{k=0}^{N-1}$ can be accomplished by calculating a few FFTs for each combination of $\{d,l\}$, requiring a total of $\mathcal{O}(D^2 N\log N)$ operations.

2) Computation of $\{Q_{k,k}\}_{k=0}^{N-1}$: From (25), we know that $Q_{k,k} = \frac{1}{\sqrt{N}} \sum_{d=-2D}^{2D} \alpha_{d,0} e^{j\frac{2\pi}{N}kd}$. We could either calculate $\{Q_{k,k}\}_{k=0}^{N-1}$ directly in $\mathcal{O}(DN)$ operations or via an IFFT in $\mathcal{O}(N\log N)$ operations since $[Q_{0,0}, Q_{1,1}, \ldots, Q_{N-1,N-1}]^t = \boldsymbol{F}^H[\alpha_{0,0}, \alpha_{1,0}, \ldots, \alpha_{N-1,0}]^t$.

3) Computation of $\{\|\boldsymbol{p}_k\|^2\}_{k=0}^{N-1}$: Recall that $\boldsymbol{p}_k = \boldsymbol{P}\boldsymbol{i}_k$ where $\boldsymbol{P} = \boldsymbol{F}^H \sum_k \boldsymbol{C}_k^H \boldsymbol{g}_k \boldsymbol{i}_k^H \boldsymbol{F}$. If $\bar{\boldsymbol{g}}_k$ is a length-N zero-padded version of $\boldsymbol{g}_k$ such that $[\bar{\boldsymbol{g}}_k]_{\langle k-D+n\rangle_N} = [\boldsymbol{g}_k]_n$ for $n \in \{0, \ldots, 2D+1\}$, then $\boldsymbol{C}_k^H \boldsymbol{g}_k = \boldsymbol{C}^H \bar{\boldsymbol{g}}_k$. This implies that $\boldsymbol{P} = \boldsymbol{F}^H \boldsymbol{C}^H \sum_k \bar{\boldsymbol{g}}_k \boldsymbol{i}_k^H \boldsymbol{F} = \boldsymbol{F}^H \boldsymbol{C}^H \bar{\boldsymbol{G}}\boldsymbol{F} = \mathcal{D}(\boldsymbol{b}^*)\boldsymbol{F}^H \bar{\boldsymbol{G}}\boldsymbol{F}$, where $\bar{\boldsymbol{G}} \in \mathbb{C}^{N\times N}$ is constructed using $\bar{\boldsymbol{g}}_k$ as its k^{th} column and, by definition, $\boldsymbol{C} = \boldsymbol{F}\,\mathcal{D}(\boldsymbol{b})\boldsymbol{F}^H$. This yields $\|\boldsymbol{p}_k\|^2 = \sum_n |b_n [\boldsymbol{F}^H \bar{\boldsymbol{G}}\boldsymbol{F}]_{n,k}|^2$. Note that $\bar{\boldsymbol{G}}$ is banded with $2D{+}1$ active diagonals. In the appendix we study matrices of the form $\boldsymbol{F}^H\bar{\boldsymbol{G}}\boldsymbol{F}$ and find that $[\boldsymbol{F}^H\bar{\boldsymbol{G}}\boldsymbol{F}]_{n,k} = \frac{1}{\sqrt{N}} \sum_{d=-D}^{D} e^{j\frac{2\pi}{N}nd} \alpha_{d,\langle k-n\rangle_N}$, where now $\boldsymbol{\alpha}_d = \boldsymbol{F}^H\boldsymbol{a}_d$ such that $\boldsymbol{a}_d$ is the d^{th} sub-diagonal of $\bar{\boldsymbol{G}}$. Thus

$$\|\boldsymbol{p}_k\|^2 \;=\; \frac{1}{N} \sum_{n=0}^{N-1} \left| b_n^* \sum_{d=-D}^{D} e^{j\frac{2\pi}{N}nd} \alpha_{d,\langle k-n\rangle_N} \right|^2 \tag{31}$$

$$= \frac{1}{N} \sum_{n=0}^{N-1} |b_n|^2 \sum_{d,l=-D}^{D} e^{-j\frac{2\pi}{N}n(l-d)} \alpha_{d,\langle k-n\rangle_N} \alpha_{l,\langle k-n\rangle_N}^* \tag{32}$$

$$= \frac{1}{N} \sum_{m=0}^{N-1} |b_{\langle k-m\rangle_N}|^2 \sum_{d,l=-D}^{D} e^{-j\frac{2\pi}{N}(l-d)(k-m)} \alpha_{d,m} \alpha_{l,m}^* \tag{33}$$

Reusing the definitions $\beta_m(d,l) := \alpha_{d,m}\alpha_{l,m}^* e^{j\frac{2\pi}{N}(l-d)m}$ and $\boldsymbol{D}(d,l) := \mathcal{D}([e^{-j\frac{2\pi}{N}(l-d)\cdot 0}, \ldots, e^{-j\frac{2\pi}{N}(l-d)(N-1)}])$, we have

$$\big[\|\boldsymbol{p}_0\|^2,\; \|\boldsymbol{p}_1\|^2,\; \ldots,\; \|\boldsymbol{p}_{N-1}\|^2\big]^t$$

$$= \frac{1}{N} \sum_{d,l=-D}^{D} \boldsymbol{D}(d,l)\,\mathcal{C}(\boldsymbol{b}\odot\boldsymbol{b})\boldsymbol{\beta}(d,l) \tag{34}$$

$$= \frac{1}{\sqrt{N}} \sum_{d,l=-D}^{D} \boldsymbol{D}(d,l)\boldsymbol{F}\,\mathcal{D}\big(\boldsymbol{F}^H(\boldsymbol{b}\odot\boldsymbol{b})\big)\boldsymbol{F}^H\boldsymbol{\beta}(d,l) \tag{35}$$

Thus $\{\|\boldsymbol{p}_k\|^2\}_{k=0}^{N-1}$ can be calculated using a few FFTs for each combination of $\{d,l\}$, requiring a total of $\mathcal{O}(D^2 N\log N)$ operations.

To conclude, the iterative symbol estimation algorithm outlined in Table 1 requires only $\mathcal{O}(D^2 N\log N)$ operations per iteration to estimate N symbols.

IV. SIMULATION RESULTS

In Fig. 4 we plot the simulated (uncoded) symbol error rate versus SNR:$= -10\log_{10}\sigma^2$ for BPSK in WSSUS Rayleigh fading channels (generated using Jakes model [13]) with uniform power delay profile and unit energy (i.e., $\sum_l \sigma_l^2 = 1$). The SCCP block length is $N = 128$ and both the channel delay spread and guard interval length are $N/4$ samples. Each trace represents results averaged from 5000 channel realizations.

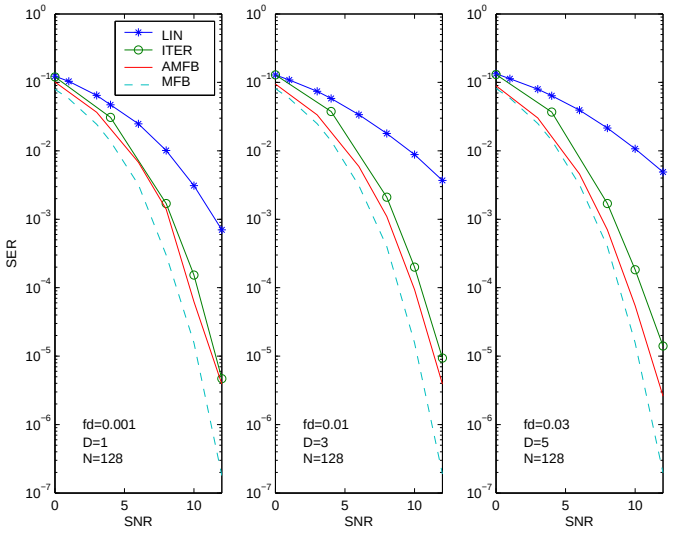

Fig. 4. Symbol error rate versus SNR after 10 iterations for $N = 128$ and WSSUS Rayleigh fading with various cases of $\{f_\mathsf{d}, D\}$.

The performance of the iterative algorithm was measured after 10 iterations and compared to joint linear MMSE estimation of $\boldsymbol{s}$ from $\boldsymbol{x}$ (see, e.g., [12]), an expensive technique requiring $\mathcal{O}(N^3)$ operations per data block, and two versions of the matched-filter bound (MFB). The *true* MFB represents the performance of the optimum detector of s_k assuming that $\{s_l, l \neq k\}$ are known. As such, it relies on the true system model (1) as opposed to the approximate model (8). We define the *approximate matched filter bound* (AMFB) to be the MFB for the approximate model (8). The AMFB lower bounds the performance of our iterative algorithm, which leverages the banded structure of $\breve{\mathcal{H}}$ for complexity reduction.

Figure 4 shows that the iterative algorithm significantly outperforms the joint linear MMSE, even though the latter will be more computationally intensive for large N. The iterative algorithm performs quite close to the AMFB, which indicates that the iterative algorithm is doing a good job of soft interference cancellation. The gap between AFMB and MFB reflects the cost of the banded approximation (8).

V. Conclusions

In this paper we presented a two-stage receiver for SCCP in doubly-dispersive channels. The first stage consists of low-complexity linear preprocessing—here taking the form of time-domain windowing—whose goal is to truncate the effective Doppler response in an SINR-optimal fashion. The second stage consists of an iterative symbol estimation algorithm which uses the results of previous iterations to perform soft interference cancellation. As with classical SCCP (and OFDM) equalization techniques, the proposed iterative receiver has an implementation complexity of only $\mathcal{O}(\log N)$ operations per symbol. Simulations suggest that the performance of the proposed receiver comes within about 2dB of the MFB, far surpassing that of the classical linear-MMSE receiver (which ignores the finite-alphabet symbol property). As the iterative algorithm evolves log-likelihood ratios, a soft decoding stage could easily be embedded (e.g., [16]) to further improve performance.

Appendix

Say $\boldsymbol{H} \in \mathbb{C}^{N\times N}$ has the banded structure of Fig. 1 but with $2PD+1$ active diagonals. Now define $a_{n,m} := [\boldsymbol{H}]_{\langle n+m\rangle_N, m}$ for $n \in \mathbb{Z}$ and $m \in \{0, 1, \ldots, N-1\}$, so that $[\boldsymbol{H}]_{n,m} = a_{n-m,m}$. The vector $\boldsymbol{a}_d := [a_{d,0}, \ldots, a_{d,N-1}]^t$ collects the elements on the d^{th} sub-diagonal of $\boldsymbol{H}$, so that $\boldsymbol{H}$ is completely described by the $2PD+1$ vectors $\{\boldsymbol{a}_{-PD}, \ldots, \boldsymbol{a}_{PD}\}$.

Examining $\boldsymbol{B} = \boldsymbol{F}^H \boldsymbol{H} \boldsymbol{F}$, we find that

$$\begin{aligned} B_{n,m} &= \frac{1}{N}\sum_{k=0}^{N-1}\sum_{l=0}^{N-1} e^{j\frac{2\pi}{N}nk} a_{k-l,l} e^{-j\frac{2\pi}{N}lm} \\ &= \frac{1}{N}\sum_{d=-PD}^{PD} e^{j\frac{2\pi}{N}nd}\sum_{l=0}^{N-1} a_{d,l} e^{-j\frac{2\pi}{N}l(m-n)} \\ &= \frac{1}{\sqrt{N}}\sum_{d=-PD}^{PD} e^{j\frac{2\pi}{N}nd}[\boldsymbol{F}\boldsymbol{a}_d]_{\langle m-n\rangle_N}. \end{aligned}$$

References

[1] S. B. Weinstein and P. M. Ebert, "Data transmission by frequency division multiplexing using the discrete Fourier transform," *IEEE Trans. Commun.*, vol. 19, pp. 628–634, Oct. 1971.

[2] L. J. Cimini, Jr., "Analysis and simulation of a digital mobile radio channel using orthogonal frequency division multiplexing," *IEEE Trans. Commun.*, vol. 33, pp. 665–765, July 1985.

[3] H. Sari, G. Karam, and I. Jeanclaude, "Transmission techniques for digital terrestrial TV broadcasting," *IEEE Commun. Mag.*, pp. 100–109, Feb. 1995.

[4] D. Falconer, S. L. Ariyavisitakul, A. Benyamin-Seeyar, and B. Eidson, "Frequency domain equalization for single-carrier broadband wireless systems," *IEEE Commun. Mag.*, vol. 40, pp. 58–66, Apr. 2002.

[5] M. Russell and G. L. Stüber, "Interchannel interference analysis of OFDM in a mobile environment," in *Proc. IEEE Veh. Tech. Conf.*, vol. 2, pp. 820–824, 1995.

[6] P. Robertson and S. Kaiser, "The effects of Doppler spreads on OFDM(A) mobile radio systems," in *Proc. IEEE Veh. Tech. Conf.*, vol. 1, pp. 329–333, 1999.

[7] Y. Li and L. J. Cimini, Jr., "Bounds on the interchannel interference of OFDM in time-varying impairments," *IEEE Trans. Commun.*, vol. 49, pp. 401–404, Mar. 2001.

[8] W. G. Jeon, K. H. Chang, and Y. S. Cho, "An equalization technique for orthogonal frequency-division multiplexing systems in time-variant multipath channels," *IEEE Trans. Commun.*, vol. 47, pp. 27–32, Jan. 1999.

[9] Y.-S. Choi, P. J. Voltz, and F. A. Cassara, "On channel estimation and detection for multicarrier signals in fast and selective Rayleigh fading channels," *IEEE Trans. Commun.*, vol. 49, pp. 1375–1387, Aug. 2001.

[10] A. Stamoulis, S. N. Diggavi, and N. Al-Dhahir, "Intercarrier interference in MIMO OFDM," *IEEE Trans. Signal Processing*, vol. 50, pp. 2451–2464, Oct. 2002.

[11] X. Cai and G. B. Giannakis, "Bounding performance and suppressing inter-carrier interference in wireless mobile OFDM," *IEEE Trans. Commun.*, 2003 (to appear).

[12] P. Schniter, "Low-complexity equalization of OFDM in doubly-selective channels," *IEEE Trans. Signal Processing*, vol. 52, pp. 1002–1011, Apr. 2004.

[13] W. C. Jakes, *Microwave Mobile Communications*. Wiley, 1974.

[14] G. H. Golub and C. F. Van Loan, *Matrix Computations*. Baltimore, MD: John Hopkins University Press, 1983.

[15] H. V. Poor, *An Introduction to Signal Detection and Estimation*. New York: Springer, 2nd ed., 1994.

[16] M. Tüchler, A. Singer, and R. Koetter, "Minimum mean square error equalization using *a priori* information," *IEEE Trans. Signal Processing*, vol. 50, pp. 673–683, Mar. 2002.